UV 380 nm Reflectivity of the Earth's Surface

J.R. Herman[1], E. Celarier[2], and D. Larko[3]

February 22, 2000

[1] Goddard Space Flight Center, Code 916, Greenbelt, MD

[2] Software Corporation of America

[3] Raytheon ITSS

Abstract 3

Introduction 4

Definition and Local Characteristics of 380 nm LER 5
Local Reflectivity Frequency of Occurrence 8

Global Characteristics of 380 nm Reflectivity 13
Global Average Reflectivity 16
Correlation with ISCCP Cloud Data 19
Global Map of Most Probable (Mode) Reflectivity 19

Annual Frequency of Occurrence Maps 22
Land Areas: 22
Ocean Areas: 23

Seasonal Frequency of Occurrence 27

Interannual Variability 27

Summary 29

References 30

Abstract The 380 nm radiance measurements of TOMS (Total Ozone Mapping Spectrometer) have been converted into a global data set of daily (1979 to 1992) Lambert equivalent reflectivities R of the Earth's surface and boundary layer (clouds, aerosols, surface haze, and snow/ice). Since UV surface reflectivity is between 2 and 8% for both land and water during all seasons of the year (except for ice and snow cover), reflectivities larger than the surface value indicates the presence of clouds, haze, or aerosols in the satellite field of view. Statistical analysis of 14 years of daily data show that most snow/ice-free regions of the Earth have their largest fraction of days each year when the reflectivity is low (R less than 10%). The 380 nm reflectivity data shows that the true surface reflectivity is 2 to 3% lower than the most frequently occurring reflectivity value for each TOMS scene. The most likely cause of this could be a combination of frequently occurring boundary-layer water or aerosol haze. For most regions, the observation of extremely clear conditions needed to estimate the surface reflectivity from space is a comparatively rare occurrence. Certain areas (e.g., Australia, southern Africa, portions of northern Africa) are cloud-free more than 80% of the year, which exposes these regions to larger amounts of UV radiation than at comparable latitudes in the Northern Hemisphere. Regions over rain-forests, jungle areas, Europe and Russia, the bands surrounding the Arctic and Antarctic regions, and many ocean areas have significant cloud cover (R>15%) more than half of each year. In the low to middle latitudes, the areas with the heaviest cloud cover (highest reflectivity for most of the year) are the forest areas of northern South America, southern Central America, the jungle areas of equatorial Africa, and high mountain regions such as the Himalayas or the Andes. The TOMS reflectivity data show the presence of large nearly-clear ocean areas and the effects of the major ocean currents on cloud production.

Introduction

The global distribution and characteristics of the Earth's clouds have been the subject of intense study for their relationship to weather and climate, and for their influence on the amount of UV radiation able to reach the Earth's surface [Herman et al., 1999; 2000; Krotkov et al., 1999, Lubin et al., 1998, and many earlier papers, see WMO, 1999]. The most complete climatology of global cloud cover has been developed from the data accumulated by ISCCP (International Satellite Cloud Climatology Project). ISCCP is a multiple-year (1982 to present) visible to infrared-wavelength data set based on a composite from a suite of weather satellites operated by several nations [Rossow and Garder, 1993a; 1993b]. Most of the data upon which ISCCP is based were obtained from a multi-satellite composite of radiance measurements at fairly high spatial resolution. The ISCCP cloud data are most accurate over water, where the surface reflectivity is small and nearly invariant both seasonally and between years. Over land, there are strong seasonal surface and geographical components that can affect the derived cloud characteristics for thin clouds (optical depth less than about 10). A related data set has been obtained by TOMS (Total Ozone Mapping Spectrometer, 1978 to present) at ultraviolet (UV) wavelengths (340, 360, and 380 nm). This data set is of lower spatial resolution (on average, about 100 km), but has the advantage that the UV surface reflectivity is low (2 to 10%) and approximately constant over both land and water (except in the presence of snow/ice). While the ISCCP data are most often presented in the form of optical depth, cloud height, and cloud fraction, the TOMS data are in the form of Lambert equivalent reflectivity, LER (see below for an operational definition). The LER combines the effects of cloud fraction, cloud height, and cloud optical depth in a manner closely related to the energy reflected back to space [Herman et al., 2000] and transmitted to the ground [Eck et al., 1987; 1995; Krotkov et al., 2000; Herman et al., 1999].

The LER of the Earth's surface and atmosphere, as calculated from satellite-observed radiances, also includes the effects of a mixture of the underlying reflectivity of the land and oceans, and the reflectivity of particulates suspended in the atmosphere (clouds, water haze and aerosols). In a previous study, the minima from each scene of the 380 nm LER over a 14-year data record from TOMS gave an estimate of the underlying surface reflectivity [Herman and Celarier, 1997]. The results showed that the snow-free surface reflectivity over land was 2 to 4%, with some areas reaching as high as 8 to 10% (e.g., Sahara Desert and phytoplankton-clear regions of the oceans, such as the large gyre west of South America at 45°S). In general, the LER is lower over the land than over the oceans (5%–8%), though both land and water have features outside of these ranges. As shown in this paper, the observation of extremely clear conditions needed to estimate the surface reflectivity from space is an infrequent occurrence.

Measured UV and visible radiances, and the underlying scene reflectivities, are used by satellites (e.g., TOMS, POLDER, GOME, SeaWiFS) for remote sensing of the amounts of ozone, aerosols, and other chemical constituents (e.g., NO_2), the detection of ocean properties (e.g., phytoplankton), and for estimates of UV irradiance at the Earth's surface. In the case of TOMS, the derived minimum LER climatology is used to identify scenes containing aerosols or sub-Field of View (FOV) clouds, and as the background reflectivity for the ozone retrieval. The

LER climatology has been used as part of the estimate for atmospheric radiative forcing when dust aerosols are present [Hsu et al., 1999] and for calculating the aerosol optical depth [Torres et al., 1998]. While the presence of extremely clear scenes is necessary for measuring certain surface and underwater properties, the use of the Earth's minimum surface reflectivity may not be the most appropriate value for satellite retrievals of atmospheric composition. Instead, the more frequently occurring scene reflectivity caused by both the surface and the presence of boundary-layer haze or aerosol should be used.

The reflectivity time series for Hudson Bay (60°N 85°W) shows that the Nimbus-7/TOMS 380 nm radiance channel is very stable [Herman et al., 2000], with a winter ice/snow/cloud reflectivity of 91±2% (without outliers) and a summer clear-sky fresh-water reflectivity of 4±1%. From the data, there is no sensible drift of the TOMS instrument, except for a small change near the end of 1992 to May 1993, where it appears that the minimum reflectivity may be biased about 2% high. Part of this bias may be associated with the heavy aerosol loading from the Mt. Pinatubo eruption in June 1991, from the satellite orbit drift (from near noon to about 10:30 am) that occurred during the last years of operation of Nimbus-7/TOMS, or from increasing problems with the on-orbit calibration during 1993.

The highly stable long-term reflectivity values and patterns are useful for understanding the causes and patterns of persistent cloud formation, for forming a baseline for estimates of UV penetration to the surface [Herman et al., 1999], and for estimates of UV and visible radiation reflected back to space using the area- and zenith-angle weighted annual global-average reflectivity [Herman et al., 2000]. In addition, reflectivity observations in the UV are almost independent of the land and ocean reflectivities (except over snow/ice), so that reflectivity changes and values over the local climatological minimum are almost always clouds, haze, or aerosols.

This paper discusses the characteristics of the Nimbus-7/TOMS reflectivity data in terms of means values (global, zonal, and local time series), most frequently occurring value (mode), and global maps of the frequency of occurrence of reflectivity values greater than or less than specified limits. The reflectivity maps are used to identify some of the underlying causes of the annual and seasonal reflectivity patterns seen in the Nimbus-7/TOMS data (November 1978 to May 1993).

Definition and Local Characteristics of 380 nm LER

The 380 nm LER is calculated by requiring that the measured TOMS radiance I_{SM} match the calculated radiance I_S at the observing position of the satellite (see Equation 1) by adjusting a single free parameter R in the formal solution of the radiative transfer equation

$$I_S(\Omega,\Theta,R,P_O) = \frac{RI_d(\Omega,\Theta,P_O)f(\Omega,\Theta,P_O)}{1 - RS_b(\Omega,P_O)} + I_{dO}(\Omega,\Theta,P_O) = I_{SM} \qquad (1)$$

where Ω = ozone amount
Θ = viewing geometry (solar zenith angle, satellite look angle, azimuth angle)
R = LER at P_O
P_O = reflecting surface pressure
S_b = fraction scattered back to P_O from the atmosphere
I_d = sum of direct and diffuse irradiance reaching P_O
f = fraction of radiation reflected from P_O reaching the satellite
I_{dO} = radiance scattered back from the atmosphere for R=0 and P=P_O

From Equation 1,

$$R = \frac{I_{SM} - I_{dO}}{I_d f + (I_{SM} - I_{dO}) S_b} \tag{2}$$

The standard tabulated TOMS reflectivities R_{PC} (available from the Goddard DAAC or from ftp://jwocky.gsfc.nasa.gov/pub/n7toms) are based on the assumption that part of the reflected radiance comes from the ground and part from cloud when 8 < R < 80%. To estimate the partial cloud fraction ρ, the radiances I_g and I_C reaching the satellite are calculated for a clear sky FOV with a surface reflectivity R_g = 8% and a cloud covered FOV with reflectivity R_C = 80% located at a cloud-height pressure corresponding to P_C. The pressure-height P_C is determined from an ISCCP monthly-average cloud-height climatology data set [Rossow and Garder, 1993a; 1993b]. If $I_g \leq I_{SM} \leq I_C$, then the fraction of cloud cover is estimated as

$$\rho = \frac{I_{SM} - I_g}{I_C - I_g} \tag{3}$$

and the effective partial-cloud reflectivity R_{PC},

$$\begin{aligned} R_{PC} &= R && \rho<1 \quad \text{or} \quad R<0.08 \\ R_{PC} &= R_g (1 - \rho) + R_C \rho = 0.08 (1 - \rho) + 0.8 \rho && 0\leq\rho\leq1 \quad \text{or} \quad 0.08\leq R\leq 0.8 \\ R_{PC} &= R && \rho>1 \quad \text{or} \quad R>0.8 \end{aligned} \tag{4}$$

When snow and ice are assumed to be present in the FOV, based on snow/ice climatology tables, it is assumed that the contribution to I_{SM} comes from an FOV containing half clear sky with highly reflective snow/ice covered ground (R_g = R) and half cloud cover over snow/ice (R_C = R) with ρ = 0.5. While the tabulated reflectivity values for R_{PC} are approximately equal to R, they are not used in either the aerosol or ozone retrievals. Instead, the 380 nm radiances (360 nm for EP/TOMS) and the cloud fraction ρ are used [McPeters et al., 1998]. The underlying reason for using ρ is to more accurately account for the calculated radiance wavelength dependence arising from Rayleigh scattering in the molecular atmosphere above and below the estimated cloud height in a TOMS FOV.

Removing the partial-cloud Rayleigh scattering effect corrects a small error in calculated ozone amounts, and a much larger error in estimating the amount of tropospheric aerosol (UV-absorbing and non-absorbing aerosols) in terms of aerosol index and optical depth [Herman et al., 1997; Torres et al., 1998]. By using R_{PC} for scenes containing clouds, but known to be aerosol free, the calculated aerosol index is zero.

If it is desired to calculate R for wavelengths λ shorter than 340 nm (331 nm for EP-TOMS), the values of R calculated from Equation 1 require that the ozone amount is known, and, for all wavelengths, that the background multiple-scattering molecular atmosphere is accurately specified. For wavelengths greater than or equal to 340 nm, the ozone amount can be ignored. R represents the equivalent scene reflectivity (the combined effect of the surface, clouds, water haze, and aerosols) after removal of Rayleigh scattering effects. R is an approximation to the angular average reflectivity, since it is based on only a small subset of the Earth's BRDF (bi-directional reflectivity distribution function) from views between $\pm 53^{\circ}$ in a direction approximately perpendicular to the principal plane.

In this paper, either R or R_{PC} could be used to estimate the approximate reflectivity of a TOMS scene. We will use the Nimbus-7/TOMS tabulated values of R_{PC} based on 380 nm measured radiances.

In magnitude, R should range from 0 to 1, but can be negative or greater than 1 if there are absorbing aerosols that are not taken into account, errors in ozone amounts for $\lambda<340$ nm, or the reflecting surfaces are sufficiently non-Lambertian (e.g., sun glint from ice or oceans). Another possibility for errors in R can occur if the phase functions of aerosols present in the atmosphere are not adequately approximated. In practice, the values of R are almost always between 0 and 1 for the near-90° azimuth angles typical of Nimbus-7/TOMS observations. Most exceptions are over regions of ocean sun glint and after injection of volcanic aerosols into the stratosphere (e.g., after the 1983 El Chichon and 1991 Mt. Pinatubo eruptions). Corrections can be applied for the volcanic effects [Torres et al., 1994; Herman et al., 1994], and for the ocean sun glint. When clouds are present, the scene reflectivity R is frequently composed of a mixture of sub-FOV clouds, surface reflectivity, and possible aerosol backscatter. The approximation of scene albedo by the LER (instead of the more complicated BRDF) is improved by having the large TOMS field of view, 50 km x 50 km to 100 km x 200 km, averaging out the effects of individual clouds or surface features.

While the ISCCP cloud height climatology data set is used in the TOMS algorithms, cloud height mainly affects the ozone retrieval and not the reflectivity calculation over clouds. The ozone-retrieval algorithm adds a climatological estimate of tropospheric ozone below the estimated height of the cloud. Over highly reflective clouds (e.g., 100>R>60%), the calculated radiance originating from Rayleigh scattering plus the cloud reflectivity is only weakly dependent on cloud height (about $\pm 2.5\%$ for clouds between 200 and 1000 mb). Over lower reflectivity clouds, the cloud-height errors in calculated radiances are smaller. There is an apparent measured correlation of reflectivity with cloud height that arises from the fact that clouds with large optical depths tend to have higher cloud-top heights.

The values of the 380 nm LER can be computed for any geographic location from the measured TOMS radiances. In the following sets of figures, examples of reflectivity data are given for different locations showing typical or extreme situations. Two typical daily reflectivity data sets over land are calculated for a scene in western Virginia (37°N) near the east coast of the US and for New South Wales (30°S) near the east coast of Australia. For purposes of illustration, but not analysis, the data set has been restricted to January 1979 to December 1987, limiting the number of displayed data points.

Local Reflectivity Frequency of Occurrence

The LER values shown in Figure 1 for eastern Australia show that there were a much larger percentage of clear days than for western Virginia (or most other land areas) over the indicated period (3285 days or 9 years, 1979 to 1987). During this period, eastern Australia had almost twice as many clear days as Virginia (1500 compared to 800 days for $R<0.1$, or $\tau<2$, and 425 compared to 90 days for $R<0.04$, or $\tau<1.2$). In addition, the mean reflectivity in Virginia is 0.32 ± 0.26 (approximate summer optical depth of 5.5) compared to the much lower value in Australia of 0.18 ± 0.19 (approximate summer optical depth of 3.3). The lowest value present in the histograms correspond to extremely clear days that are almost free of both clouds and ground haze. These clear-sky data are suitable for estimating the surface reflectivity [Herman and Celarier, 1997]. The value of R is related to the equivalent plane-parallel cloud optical depth τ that varies with wavelength, solar zenith angle, and satellite zenith angle [Herman et al.,1999; Krotkov et al., 2000].

An important consequence of the lower mean reflectivity and increased number of clear-sky days is the increased level of UV exposure in Australia relative to that in Virginia [Herman et al., 1999]. The high level of UV exposure in Australia is known to present a serious public health problem with skin cancer. The same statistical results are observed in the entire 14-year Nimbus-7/TOMS data record, but are harder to show graphically in Figure 1 because of the increased density of points.

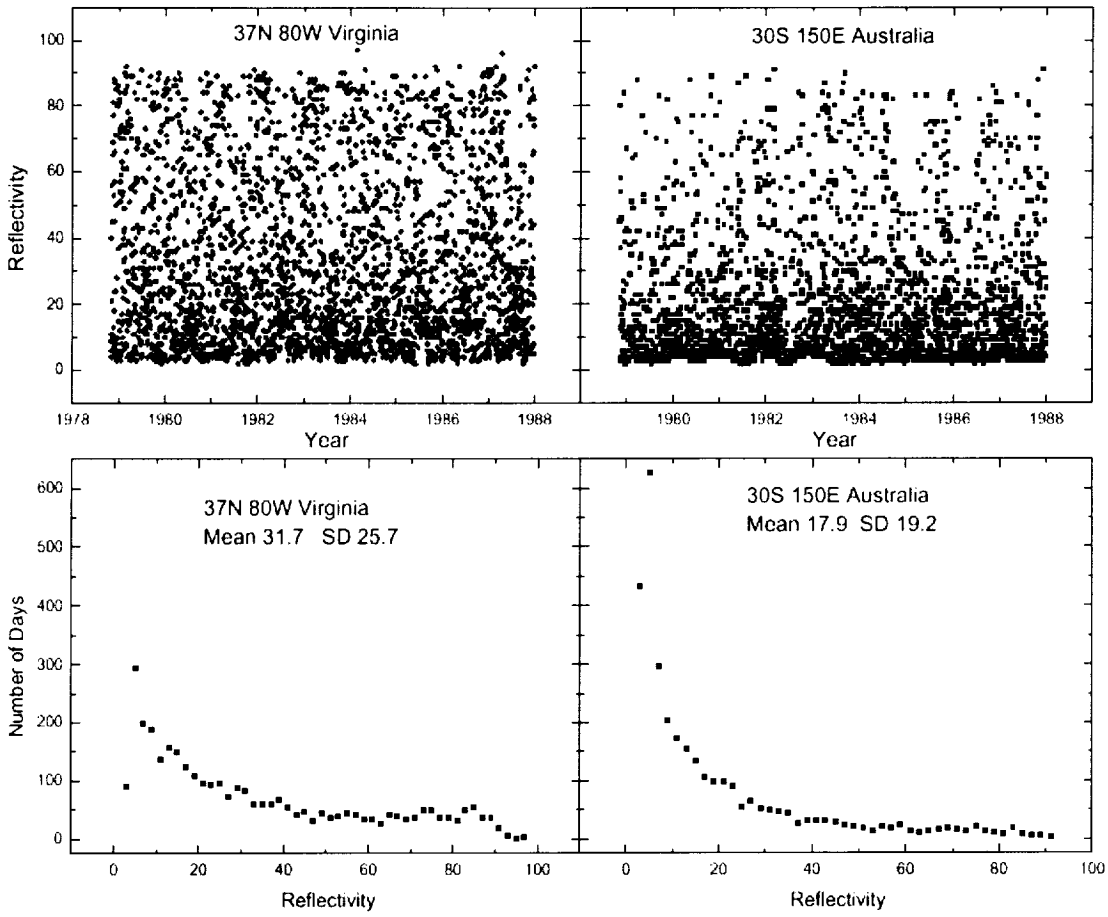

Figure 1 The values of reflectivity (1979 to 1988) and their frequency of occurrence over eastern Australia and central Virginia, USA. Reflectivities are represented in percent (0 to 100). In this and subsequent figures, the reflectivity bins are 2% (ΔR=0.02).

The statistical characteristics (e.g., mean, mode, frequency of occurrence) of the observed LER values vary widely for different geographical locations. For example, Figure 2 shows the reflectivity for central Europe where the proportion of cloudy days is large compared to many regions of the world. Western Nevada, known for large numbers of sunny days, is far closer to the conditions in Australia than conditions in relatively cloudy Virginia. Another extreme case is for observations, with and without clouds, over a permanent ice sheet such as that occurring in Greenland. Here the mean reflectivity is 94±5%, with most days having R>85%. Except for coastal areas of Greenland, these values are typical for the permanent ice sheet. In regions of the world where the snow/ice cover changes daily or from week to week, there is no way for TOMS to distinguish cloud reflectivity from that for snow/ice.

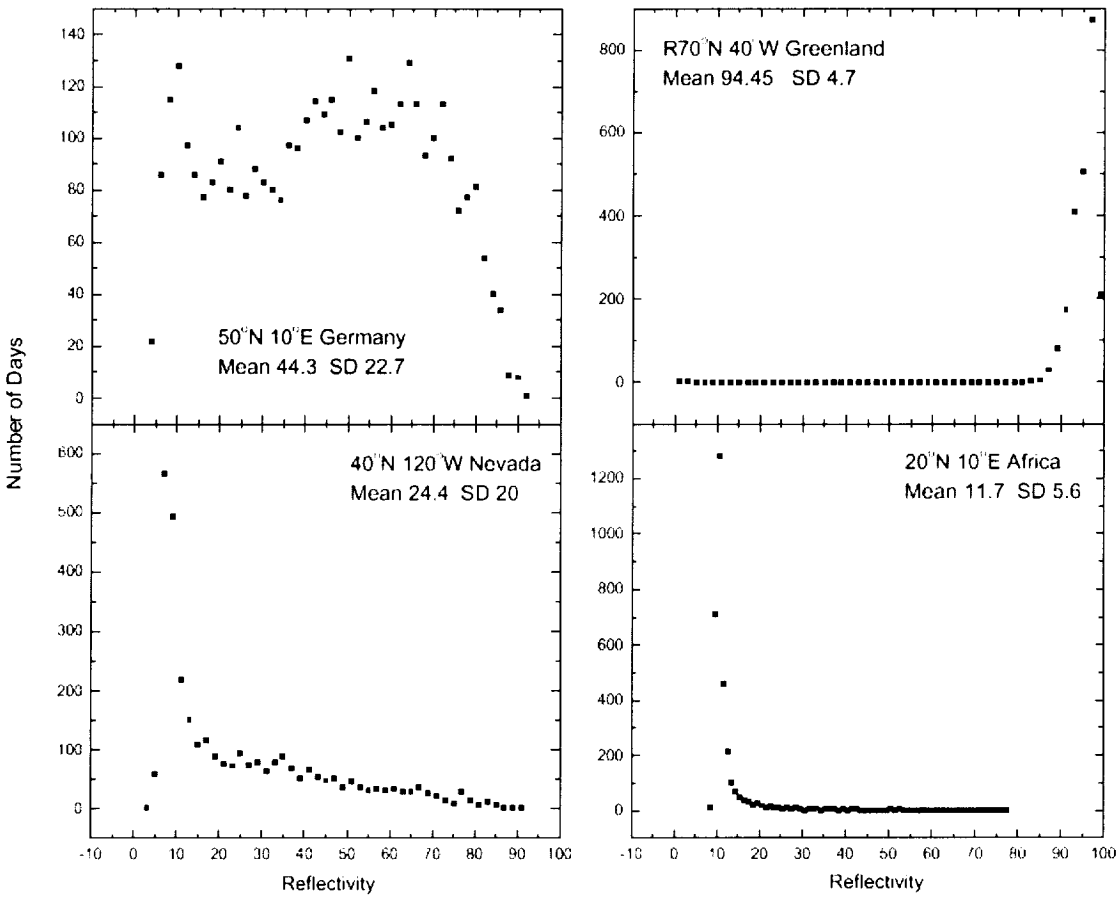

Figure 2 The frequency of occurrence of different reflectivity values at locations in Germany, Nevada, Greenland, and in Niger. Reflectivity expressed in percent.

A clear-sky extreme occurs in central Africa, in Niger northeast of Lake Chad, where the frequency of occurrence of cloudiness is quite small. In Niger at 20°N 10°E , the most common reflectivity value is 10%, with a minimum value of 8-9%, consistent with the observations of the nearly continuous presence of tropospheric dust plumes over a sandy surface for 10 months each year [Herman et al., 1998]. Dust plumes tend to darken the scene by 2 to 3% relative to the clear-sky surface reflectivity (aerosol-free conditions occur most often in December). Lybia, which has a bright sandy surface, but much less frequent occurrence of tropospheric dust plumes, has a surface reflectivity of about 10 to12%, one of the highest surface albedo regions without snow or ice. There are small regions with even higher land reflectivity (e.g., White Sands National Monument, New Mexico), but these are too small to show up on the TOMS 100 km x 100 km footprint.

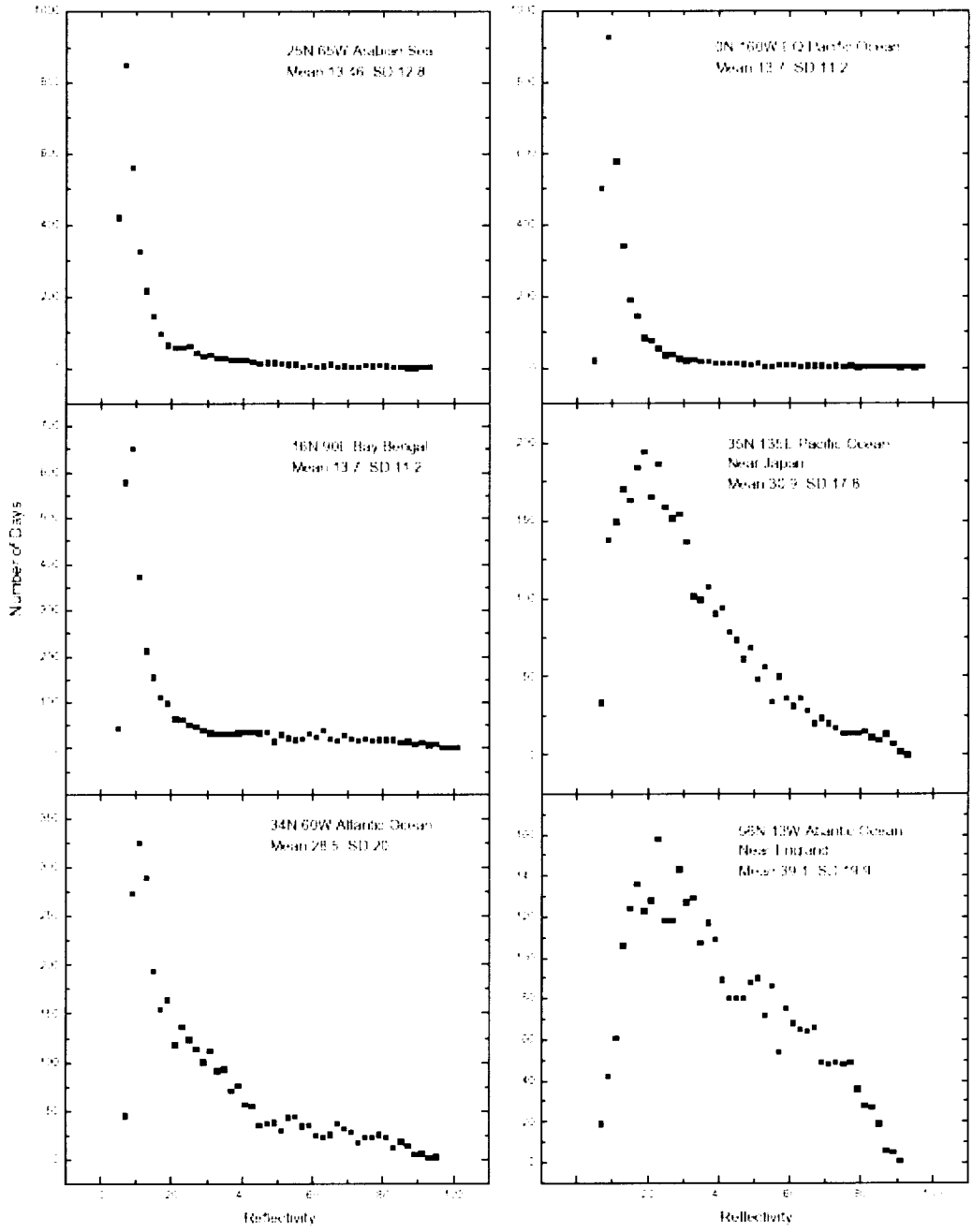

Figure 3 Frequency of occurrence of reflectivity values over ocean areas.

The low-reflectivity mode values vary between locations depending on the local meteorology and the presence of aerosols or haze. For relatively clear-sky locations, (e.g., Nevada and Australia), the majority of days have a reflectivity of 15% or greater, indicating scenes containing thin or broken clouds. Aerosols in cloud-free scenes can produce 380 nm

reflectivities up to about 15% including the surface reflectivity. The global distribution of mode values and frequency of occurrence data is presented later.

The degree of cloudiness over various ocean areas can differ significantly (see Figure 3). The Bay of Bengal, Arabian Sea, and the equatorial Pacific Ocean have large numbers of clear days when the reflectivity is 10% or less and very few completely cloudy days when the reflectivity is 50% or greater. This is quite different than the Mid-Atlantic Ocean where there are a substantial number of cloudy days. Similarly, the Pacific ocean region near Japan and the Atlantic Ocean near England show a large number of days when it is cloudy (R>50%). In the Atlantic, the cloud amounts are increased as a result of the warm Gulf Stream waters interacting with the cold air during the winter months.

The high reflectivity values, R>91%, of clouds over snow/ice are matched by infrequently occurring thick clouds over various land areas and oceans. Two examples of this are shown in Figure 1 for Virginia and Australia, where the reflectivity is occasionally about 90%. These values correspond to optically thick clouds that usually have their top surfaces at high altitudes and can cover large areas.

Zonal Average Reflectivity

The annual and zonally averaged reflectivity data for 14 years (1979 to 1992) has a minimum near the equator of about 22% (including an average 5% surface reflectivity) and a maximum near the poles corresponding to both increased cloudiness and snow/ice cover (see Figure 4). In the middle latitudes (~40°), the average reflectivity is about 30%, with the highest values occurring in the winter and spring. From 25°N to 55°S the seasonal amplitude is less than ±5%. The seasonal variation of R increases at higher latitudes in the Northern Hemisphere (±8% at 45°N and ±13% at 65°N. In both hemispheres, the annual amplitude deceases at very high latitudes (80° to 90°) where ice and snow are present for much or all of the year. The 85±10% SH and 80±20% NH annual modulation is caused by the difference between clear skies (lower reflectivity) and clouds over snow (higher reflectivity). There are 2 small decreases (5%) in the zonally averaged zonal-mean reflectivity near ±20° that coincide with regions containing downward air motions associated with the Hadley cloud-cell structure. **(Check with Larko)**

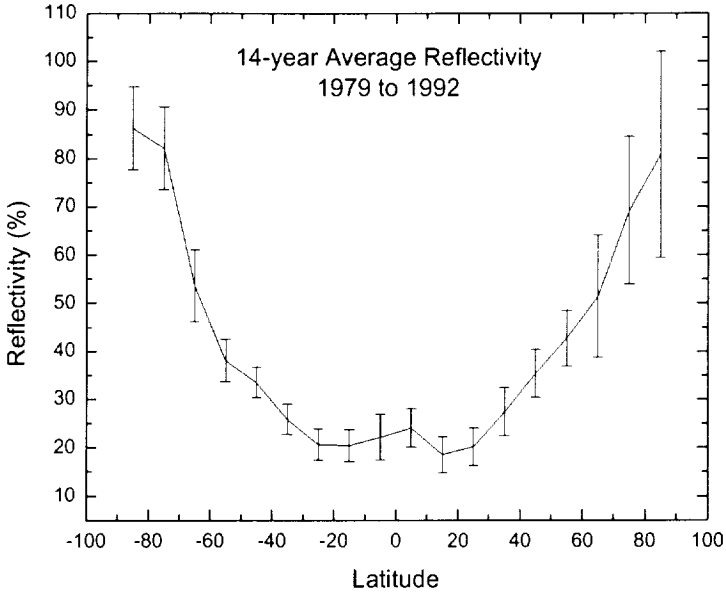

Figure 4 The 14-year zonal-average reflectivity. The error bars are 2 standard deviations.

Global Characteristics of 380 nm Reflectivity

As defined by Equation 1, The TOMS LER will detect ground reflectivity, water-ice clouds, pure scattering aerosols, and UV absorbing aerosols. The surface reflectivity (2 to 10%) combined with most aerosols have 380 nm reflectivities less than 20%. This can be seen in Plate 1, where both the aerosol index [Herman et al., 1997; Torres et al., 1998] and reflectivity are plotted together (top) and the reflectivity alone (bottom). Over northern Africa, the ground reflectivity in the desert areas is about 8 to 10% [Herman and Celarier, 1996] with dust aerosol plumes in a band from 10° to 30°N for 10 months of the year. These dust plumes tend to lower the 380 nm scene reflectivity below that of the ground [Torres et al., 1998], while smoke plumes (e.g. in South America) are brighter than the ground.

Since the LER is a single channel measurement, it cannot reliably distinguish between clouds, haze, and aerosols, but instead is a measure of the total scene reflectivity. The presence of aerosols can be distinguished from clouds using a 2 wavelength radiance analysis (e.g., 340 and 380 nm) to obtain the aerosol index (AI), as shown in the top half of Plate 1 [Herman et al., 1997]. Here the AI is computed separately with no cloud screening and superimposed over the reflectivity data. As can be seen by comparing the top and bottom halves of Plate 1, some of the aerosol plumes appear as if they were clouds. Similar difficulties occur for satellite instruments using visible channels (e.g., AVHRR) with a cloud screening procedure (based on reflectivity) to detect aerosols. For AVHRR, the cloud screening procedure based on a reflectance threshold can lead to omission of thick aerosol plumes, especially over bright land surfaces. When UV

transmission to the ground is considered, the UV-absorbing aerosols and clouds (including scattering aerosols) can be treated separately [Herman et al., 1999] unless they are mixed together within a cloud [Krotkov et al., 2000]. In this case, the aerosol index may indicate the presence of aerosols over a bright background that could be cloud or snow/ice [Hsu et al., 1999] in appropriate geographical regions and seasons.

When clouds (R>15%) and aerosols (AI>0.2) are observed that are apparently in the same or adjacent scenes, the aerosols can be seen to follow the same winds as the nearby clouds. Similar views from other days show that this is the usual situation at most locations where there are smoke or dust aerosols. The implication is that the clouds and aerosol plumes are usually, but not always, at approximately the same height [Allen et al., 1999]. Aerosol-plume trajectory modeling, using temperature derived wind fields, shows that the height of the plumes can be specified to within ±0.25 km using the altitude resolution of wind shear features in the model. The most common altitude for aerosol plumes, when far from their source on the ground, is about 3 km. Plume heights range from near the surface to about 6 km (e.g., during the summertime over the Sahara), and occasionally higher over mountain terrain.

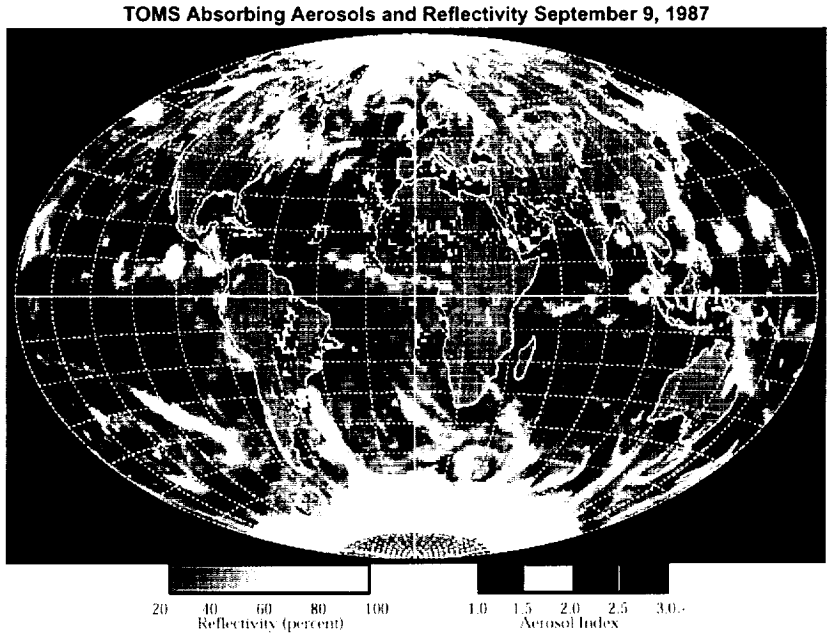

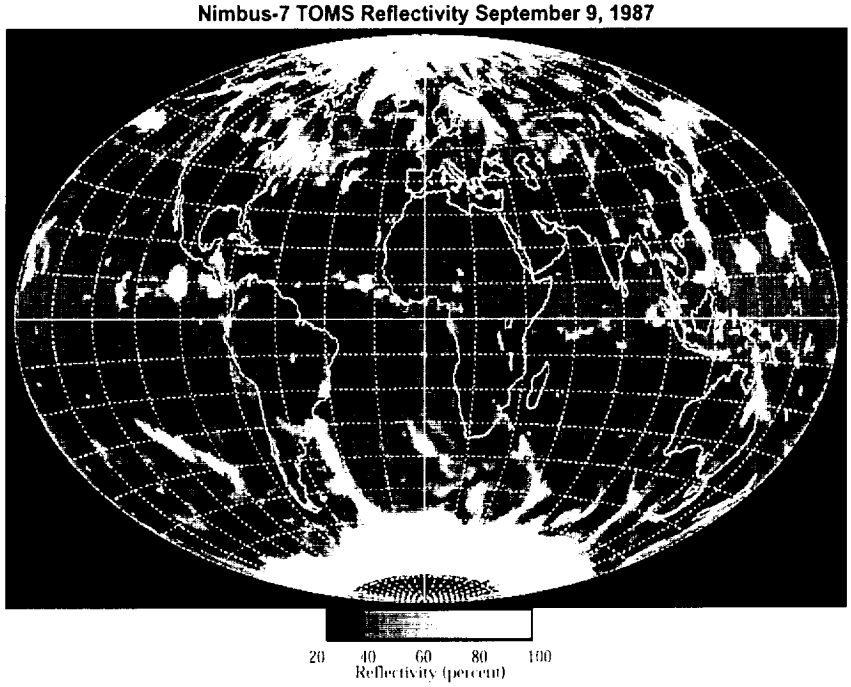

Plate 1 TOMS reflectivity and aerosol index for 09 Sept 1987. The blue and tan colors represent water and land. The upper panel has the aerosol index superimposed on top of the reflectivity data, while the lower panel is just the reflectivity data.

Global Average Reflectivity

In the absence of clouds and aerosols, the 380 nm LER of the surface is mostly dependent on the type of surface material and not on location [Herman and Celarier, 1997]. In the absence of snow/ice, the largest cause of clear-sky surface-reflectivity variation is the from the type of land (vegetated or desert), or whether the ocean water contains large amounts of absorbing material (e.g., phytoplankton) for 380 nm radiation. The geographic and seasonal variation caused by clouds and aerosols is much larger (see Plate 2) than that caused by land and ocean surface properties. While the daily 380 nm reflectivity maps show the details of individual clouds and their motions when viewed in sequence, the monthly averages for 14 years, 1979 to 1992 (see Plate 2) show distinct patterns related to persistent global wind systems, ocean currents, and major surface features such as regions of snow and ice. Note that there is missing LER data for the Arctic (January) and Antarctic (July) when sunlight is not present at the surface.

In the following sections, results are presented from UV data that parallel well-known features of clouds seen at visible wavelengths. In this discussion, the measured radiance data is converted to reflectivity so as to eliminate the seasonal and latitude solar zenith angle dependence when clouds are present, and to combine the effects of cloud optical thickness and cloud fraction. Since the TOMS instrument was stable, long-term averages can be formed to represent seasonal and annual patterns in reflectivity, and to look for long-term changes in reflectivity [Herman et al., 2000].

Regions with low average reflectivity, 12 to 24%, are present mostly over the oceans and over some land areas (see Plate 2). The largest of the persistently clear-sky land areas is the region over the Sahara extending eastward over the Arabian Peninsula, and into Pakistan and western India. The second large region is in the Southern Hemisphere, extending over Australia and Southern Africa. There are other smaller regions of low reflectivity (clear skies) over land that occur for just part of the year (e.g., during July over Brazil and Argentina, and in the summertime western US and Canada).

Regions with persistent high reflectivity, R>40%, are mostly at high latitudes in both hemispheres. The high reflectances in these regions arise from the presence of snow and ice, and two large belts of clouds near the Arctic and Antarctic regions that circulate from west to east. Over land, the cloud belt (and snow/ice) affects the reflectivity over Canada, northern US, and most of Europe and Russia, but with a strong seasonal dependence. In the US and Canada, it is relatively cloudy during the winter months compared to the summer months, with heavy banks of clouds from Pacific Ocean weather systems extending from Canada into Seattle and Oregon, and from continental weather systems producing high reflectivity down the east coast into Maryland and Virginia, R~50%. The winter east-coast reflectivity patterns are partly increased cloudiness and partly from the presence of snow/ice.

The seasonal cycle of reflectivity (clouds and snow/ice) at high and mid latitudes is stronger in the Northern Hemisphere (NH) than in the Southern Hemisphere (SH) because of the different distribution of land. The SH has almost no land, other than Antarctica (-70° to -90°), south of -50° compared to mostly land in the NH north of +50°. In both hemispheres, the winter cloud belt extends from very high latitudes to about 45°, with part of the higher NH reflectivity from underlying snow/ice.

Also present are the seasonal reflectivity variations associated with the presence of major cold-water ocean currents, such as the California current at 10° to 40°N, 120° to 140°W, the Humboldt (or Peru) current with cloud effects near the coasts of Peru and Chile, the Benguela current off of the southwest coast of Africa, and the North Atlantic Drift fed by the warm-current Gulf Stream. The effect of the California Current on cloud formation is strongest during the summer months, and fades during the spring and autumn months.. There is a relatively clear region, R~15%, in the equatorial Pacific Ocean, 10°S 120°W, where the ocean currents associated with the periodic El Nino effect appear. Just to the north, ~9°N, is a permanent narrow belt of clouds, R~33%, extending from Africa over the Atlantic and Pacific Oceans, that is part of the ITCZ (Inter-Tropical Convergence Zone) cloud system. While the ITCZ moves north and south seasonally, the position of the permanent cloud belt over the Pacific Ocean is caused by surface winds directed slightly north of the equator by South American land features, while over the Atlantic Ocean, it is nearly coincident with the equator.

There is also a seasonal high reflectivity area near the equator over heavily vegetated jungle areas (e.g., in Brazil and equatorial Africa). In Brazil, this corresponds to the occurrence of a long cloudy rainy season with clearing in June-July, drying out in August, and then having large fires with smoke during the dry season in September (see Plate 1). By October, the rain and clouds start again. Similar cloud patterns appear over equatorial Africa, Indonesia, and India, but with maximum cloudiness occurring in June and July (corresponding to the Monsoon season in India). Over India, the cloud pattern extends northward to about 40° and lasts until about October. Some areas are largely cloud free most of the year. The largest land-area examples are the Sahara, Arabian Peninsula, Southern Africa, and Australia.

Extending northward from the high southern-latitude cloud belt is a standing wave pattern to the downwind side of South America as well as another peak in the mid Pacific Ocean to the west of South America. There is no corresponding feature for Africa and Australia, probably because they do not extend far enough to the south to interfere with the general west to east cloud circulation pattern. There is a similar pattern in the Northern Hemisphere where there are downwind extensions southwards into the Atlantic along the east coast of North America and into the Pacific on the east coast of Russia and China.

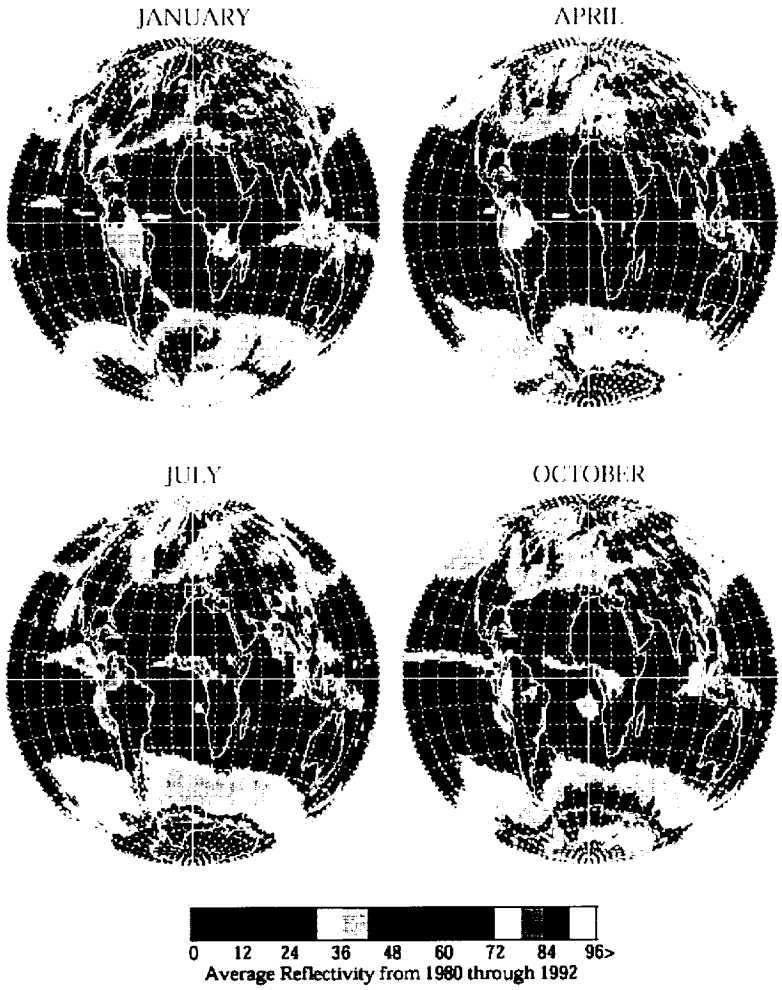

Plate 2 Monthly average reflectivity in percent for the years 1979 - 1992 for January, April, July, and October. Note that these and the following plates are full-globe views for 360° of longitude.

Correlation with ISCCP Cloud Data

ISCCP is a multiple-year (1982 to present), visible to infrared-wavelength, radiance data set based on a composite from a suite of weather satellites operated by several nations [Rossow and Garder, 1993a; 1993b]. It is frequently expressed in the form of optical depth, cloud fraction, and cloud height [Rossow, 1993c]. As such, ISCCP data cannot be compared quantitatively with TOMS reflectivity, but both data sets should show similar major features. The calculated TOMS reflectivity (1978 to present) is a combined measure of the ISCCP parameters, but for UV wavelengths. In general, the 380 nm TOMS reflectivity increases with increasing cloud optical

depth (see Figure 5), cloud fraction, and apparently with cloud height. The cloud-height correlation with reflectivity assumes that the cloud optical depth increases with increasing cloud height (geometrical thickness) for a fixed cloud fraction in the satellite FOV. This is not true for generally thin high-altitude clouds, where both the cloud base and cloud top are at high altitudes.

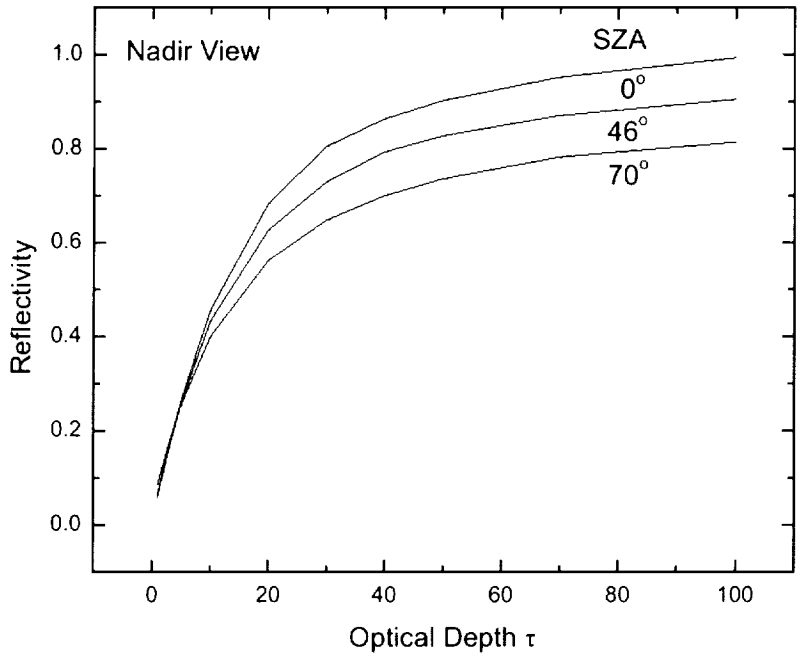

Figure 5 The relationship between cloud optical depth τ and reflectivity R for a uniform cloud field viewed from the nadir observing position from the satellite. The curves are for 3 solar zenith angles, 0, 46, and 70 degrees.

Maps showing reflectivity (see Plate 2) and frequency of occurrence of clear days, based on the 380 nm LER, show similar features to those in the 2-year average ISCCP cloud optical thickness maps [Rossow, 1993c], and, to a lesser degree, with the ISCCP cloud fraction data. The clear-scene areas in the equatorial Pacific (100°W to 180°W shown in Plate 1) match with the low ISCCP optical-depth areas (τ_I = 2 to 4). Other similar low optical depth areas, correlated with clear skies, appear in both data sets: in the southern Carribean extending eastward in to the Atlantic, off of the eastern coast of South America near 5°S, and on the east coast of Africa from the Arabian Sea to Madagascar. A very clear region in Sudan and Egypt (R<15% for nearly the entire year) correlates with $\tau_I < 4$ and an ISCCP cloud amount of less than 10%. Other regions, such as the very clear areas over Australia and southern Africa, correlate with both the ISCCP below average optical depth (4 to 8) or below average cloud amount (20 to 40%). An extremely clear area near the coast in Namibia correlates with the very low ISCCP optical depth (2 to 4). A cloudy region (less than 40 days per year with R<15%) in southern China and northern Indochina correlates with $\tau_I > 16$. Similarly, the area over middle and northern Europe, $\tau_I > 16$ correlates with a region of fewer than 40 days per year with R<15%.

Global Map of Most Probable (Mode) Reflectivity

Most areas of the Earth have frequency of occurrence distributions of 380 nm reflectivity that resemble those in Figures 1, 2, and 3. There are 2 basic types of distributions depicted, those with a single sharply defined maximum, and those with multiple local maxima, such as for Germany. If the range of reflectivities is restricted to R<30%, then for almost all regions there is a unique low-reflectivity maximum (mode) for each TOMS 1°x1.25° scene (see Plate 3). Except where there are areas with persistent clouds (e.g., Brazilian rain forest areas), the geographic mode-reflectivity patterns resemble those obtained previously for the surface reflectivity climatology [Herman and Celarier, 1997]. The chief difference is that the most probable scene reflectivities (mode) in Plate 3 are a few percent larger than the surface reflectivity. The mode values contain the reflectivity of the underlying surface, the most frequently occurring levels of ground-haze (aerosols and water haze), and for the higher values, some level of cloud contamination. Because of the 100 km spatial resolution, it is possible for the low-reflectivity mode values to contain slight cloud contamination having a reflectivity of less than 2 to 3 %.

Many land areas have a low-value mode reflectivity of 4 to 6% over an underlying surface reflectivity of 2 to 4%. The Saharan region of Africa, and extending eastward through parts of India, have mode reflectivities from 8 to12% caused by the presence of sand (more reflective than vegetated soils) and wind-blown dust [Herman et al., 1996]. The Mediterranean Sea, which has a low surface reflectivity (~5%) has a mode reflectivity of 8 to 10% because of the frequent appearance of water haze and dust aerosols. UV absorbing mineral-dust aerosol plumes appear darker than the desert land, but brighter than the water.

Other land or near-land areas have mode reflectivities of 8 to 10% (light blue) that correspond to the presence of haze and/or light clouds. Typical for this kind of region is the frequency plot shown for Germany (see Figure 2) where there is a local peak (R<15%) corresponding to haze and possibly some light cloud cover, and then a broad distribution of reflectivities up to about R~80%. The ocean area near the southwestern coast of North America (e.g., near La Jolla, California) is well known for the frequent occurrence of morning fog that dissipates into light haze by late morning and then clears in the afternoon. TOMS viewed this area between 10:30 a.m. and noon (most often near 11 a.m.) and seems to have detected this haze region (R~9%) as well as the underlying surface reflectivity on exceptionally clear days. The heavily vegetated areas in near-equatorial Central America, South America, Africa, and Indonesia have higher mode values, 24 to 28%, than other land areas because of frequently occurring clouds during the rainy season.

Reflectivity Value of Maximum Occurrence for the period 1980 through 1992

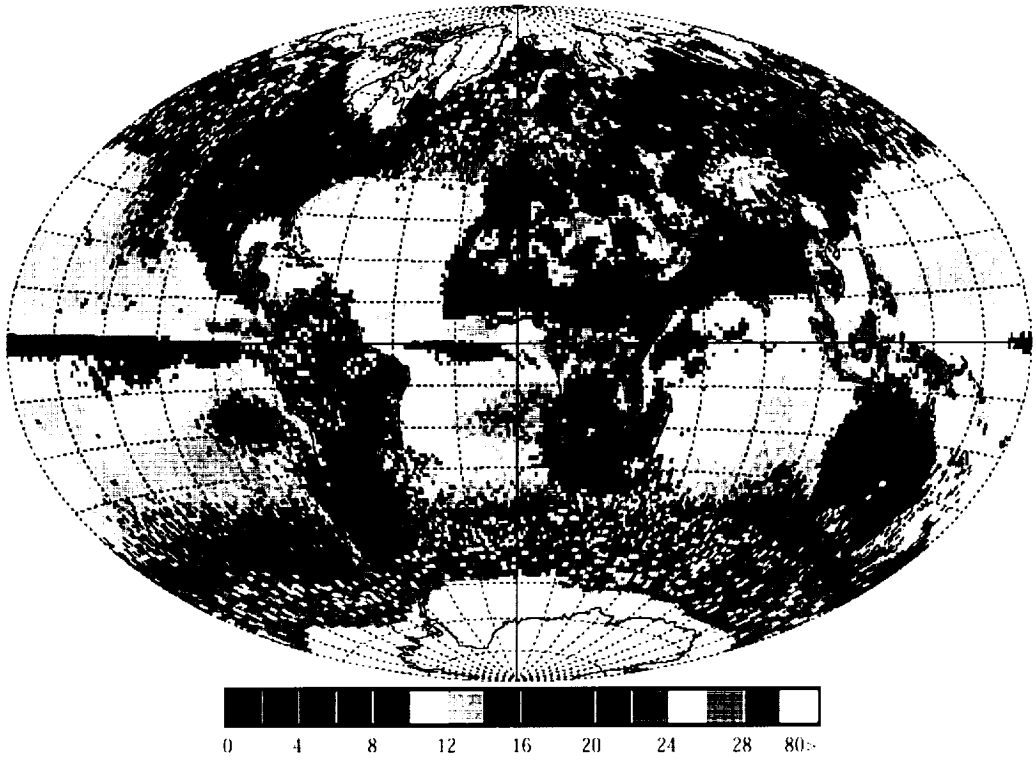

Plate 3 The global and seasonal distributions of the most probable annual value of reflectivity (mode) for each TOMS scene on a 1° x1.25° grid for values of R between 0 and 30%. All values over 30% are in the last color box (white). The most probable value corresponds to the large maximum in the reflectivity histogram (see Figures 1, 2, and 3)

Similarly, most ocean areas have mode reflectivities of 8 to14% over an underlying ocean-surface reflectivity range of 4 to 8%. There are regions of persistent cloud cover, or snow and ice, at latitudes above 40° in both hemispheres. For example, at 55°S, the average and mode reflectivities are approximately equal, 41%, with a standard error of 18%. At 55°N 15°W over the Atlantic Ocean between North America and Europe the mean reflectivity is 40±20% and the mode is 22%, with the mode being more variable than the mean. These are typical values for the cloud bands at high latitudes over ocean. At lower latitudes, there are cloudy regions located over the large ocean currents where there is temperature contrast in the water (e.g., the California and Humboldt currents and the Atlantic Ocean Gulf Stream). On the annual average basis shown in Plate 3, the Gulf Stream causes clouds to form along the eastern seaboard of New England and Canada and across the Atlantic to England and Scandinavia.

Annual Frequency of Occurrence Maps

The TOMS 380 nm LER data can be organized into the number of days per year that a particular range of reflectivity values occurs. Plate 4 shows the frequency of occurrence map (FOM) for clear days when the reflectivity is either less than 10% or less than 15%. Use of the 10% reflectivity cutoff value, to show areas with extremely clear skies, can lead to a few anomalies. For example, most of Lybia appears to have no days when the reflectivity is less than 10%, but almost 3/4 of the year with reflectivity less than 15%. This is consistent with high values of surface reflectivity (~10%) and relatively few days with thick dust clouds compared to the areas nearer to Lake Chad. Note that in this representation of reflectivity, the dark colors mean more cloudy days and the light colors, more clear days per year.

Land Areas:

Among the most prominent features of the frequency of occurrence maps are the large regions in Africa and Australia where there are a large number of extremely clear days. In Africa the largest number of clear days is associated with the dust-belt region of dry sandy soils (centered on 20°N). This belt extends from the west coast of Africa into Pakistan and parts of northern India. As with Lybia, there are portions of Arabian Peninsula that have soil reflectivities higher than 10% accompanied by clear skies so that the reflectivity is less than 15% for most of the year. In addition to the dust-belt region, there is a large area that has almost continuously clear skies (R<15%, and for about half the year with R<10%) extending down the east coast of Africa from the Arabian sea to the west coast of Madagascar.

Large parts of Australia and southern Africa have extremely low reflectivities (lack of clouds and haze) for most of the year because of elevation and extreme dryness. In western South Africa, southern Namibia, and central and western Australia, the reflectivity is less than 10% for more than three quarters of the year. The clearness of the atmosphere is responsible for the very high levels of exposure to UV radiation in these regions [Herman et al., 1999].

The Indonesian islands tend to have cloud formation from rising air forced upward by the mountains. These clouds are trapped and persistent, leading to cloud cover of at least 15% reflectivity for 300 days out of the year. A similar phenomenon occurs for Madagascar where the clouds form on the eastern side of the island, but leave the western side with clear skies for almost the entire year.

These clear dry areas are in contrast with the regions in Brazil and equatorial Africa where the cloud cover is frequent (clear days with R<10% less than 50 days per year). The southern half of South America is relatively clear (R<15%) for half the year with Argentina near Buenos Aires having very clear skies (R<10%) for half the year. Europe and parts of North America have very few low reflectivity days per year. Part of the reason is the presence of snow throughout central Europe and Russia for many days of the year, but also because there is a persistent pattern of cloudiness, especially during the spring and autumn. The US, particularly the western US, has far more clear days than Europe, with parts of New Mexico and Arizona (as

well as Mexico near the Baja and Gulf of California) nearly as clear as Australia. Northern Canada and Europe have clouds much of the year (high reflectivity) as part of one of the large belts of cloudiness that circles the globe at high latitudes in both hemispheres.

The LER for areas at higher latitudes in North America, Europe, northern China, Mongolia, and Russia is affected by the presence of snow for a significant fraction of the year. In North America this can be easily seen where the snow region extends down into the Eastern and Midwestern United States and into the Rocky Mountains. Of course, Greenland, northern Canada, northern Russia, the Arctic, and Antarctic have high reflectivities caused by either permanent ice cover or snow cover for more than half of each year.

Ocean Areas:

The most prominent features seen on Plates 4and 5 are those associated with the major ocean currents. The ocean area just west of the North America (Canada, US, Mexico) has a relatively cloudy area (dark blue or 75% cloudy days per year with R>15%, but only 30% of days with R>40%) caused by the cold water of the clockwise California current (between 120° and 135°W and 20° to 40°N) interacting with the warm summer air. On either side of this current there is less cloud formation (50% cloudy days per year with R>15%). A similar phenomenon occurs in the Southern Hemisphere, near Chile and Peru, where the cold-water counter-clockwise Humboldt current come up the western coast of South America and forms clouds during the summer. The cloud bank that forms off of the coast of Chile and Peru has increased in reflectivity since 1979 [Herman et al., 2000], suggesting that the underlying ocean current has also changed. Just to the west of this region, near the equator, is one of the least cloudy ocean regions (see also Figure 3), where it is clear (R<15%) for more than 3/4 of the year. This is also the ocean region where changes in the currents are associated with the El Nino weather pattern.

Average Number of Days per Year where Reflectivity < 15% for 1980 through 1992

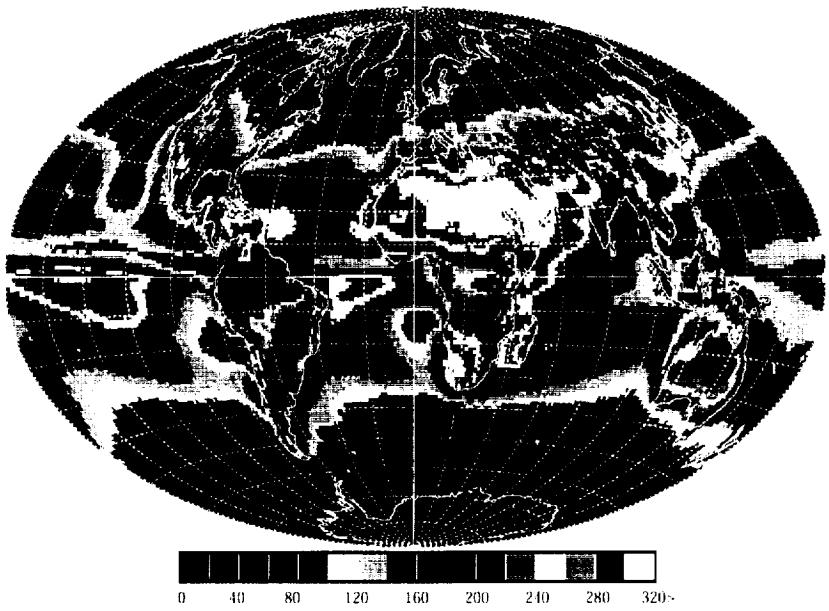

Average Number of Days per Year where Reflectivity < 10% for 1980 through 1992

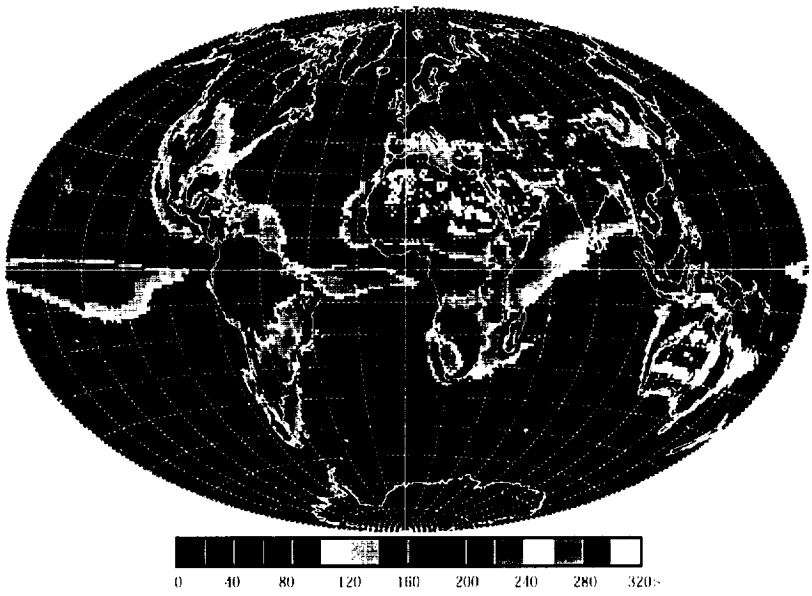

Plate 4 The areas of the Earth where there are at least an average of 20 cloud-free days per year (i.e., reflectivity less than 10%, bottom, or 15%, top). Areas colored red are cloud free about ½ the time.

At high southern latitudes, a belt of clouds (R>40% for about 1/3 of the year) moving from west to east circles the globe at latitudes greater than 40°S. A similar band circles the globe above 40°N also moving from west to east. In the equatorial and sub-equatorial regions the cloud motions are reversed, with the motions largely from east to west. Plates 4 and 5 show a geographically thin band of cloud (R>40% for 1/3 of the year and R>15% for 2/3 of the year) over the Pacific at about 9°N, and with a weaker band of cloud over the Atlantic at the same latitude. On either side of this band are relatively clear areas in both the Atlantic and Pacific (15%<R<40% for most of each year). From the LER data, there appears to be a band of clouds (R>40% for more than 1/3 of the year, Plate 5) extending northward from the sub-Antarctic cloud band, across South America on the eastern side of the Andes, and connected to the thin cloud band at 9°N.

Plate 5 illustrates the areas of the Earth having high reflectivity scenes optically thick cloud cover, or snow and ice, for 4 different reflectivity cutoff values (R>40, R>50, R>60, and R>70%) that are present for at least 12% of the time, or about 44 days per year (purple). For latitudes within the Arctic or Antarctic circle, the scale for percentage of the year is normalized to the number of sunlit days. Clearly visible in Plate 5 are the Antarctic continent (white) and the ice shelf (pink through blue) from September to March. The ocean edges of the Antarctic ice sheet have high reflectivity for about 50% of the sunlit portion of the year. During the summer months, much of this region melts into a mix of open water and icebergs. This region has also increased in reflectivity since 1979 indicating an increase in the mix of clouds and/or ice [Herman et al., 2000]. In the Arctic and Greenland, the permanent ice sheets are visible as white. Moving southward, these areas are represented by darker colors as the ice cover melts during a portion of the summer. For example, Hudson Bay has R>60% about 50% of the year (red) and R>40% for 80% of the year, even though there is open water with much lower reflectivity (R~4%) during the summer months (see Herman et al., 2000).

Examining the daily reflectivity maps in a rapid sequence reveals a number of persistent flow patterns that are also seen in the annual, seasonal, and monthly frequency of occurrence maps. The dimension of the cloud features (high-reflectivity features) is from 50 km (minimum size seen by TOMS) to about 1000 km, and sometimes larger. The R>40% map (Plate 5) shows a standing wave pattern near the southern portion of South America, with two peaks near 150°W and 40°W. Clouds are pulled off of the high-latitude west to east (westerly) flow into a northerly flow up the east side of the Andes mountains where the clouds connect with the general easterly flow in the tropical regions. Similar flow patterns are seen in other midlatitude regions and follow the persistent features shown in the seasonal and yearly occurrence maps.

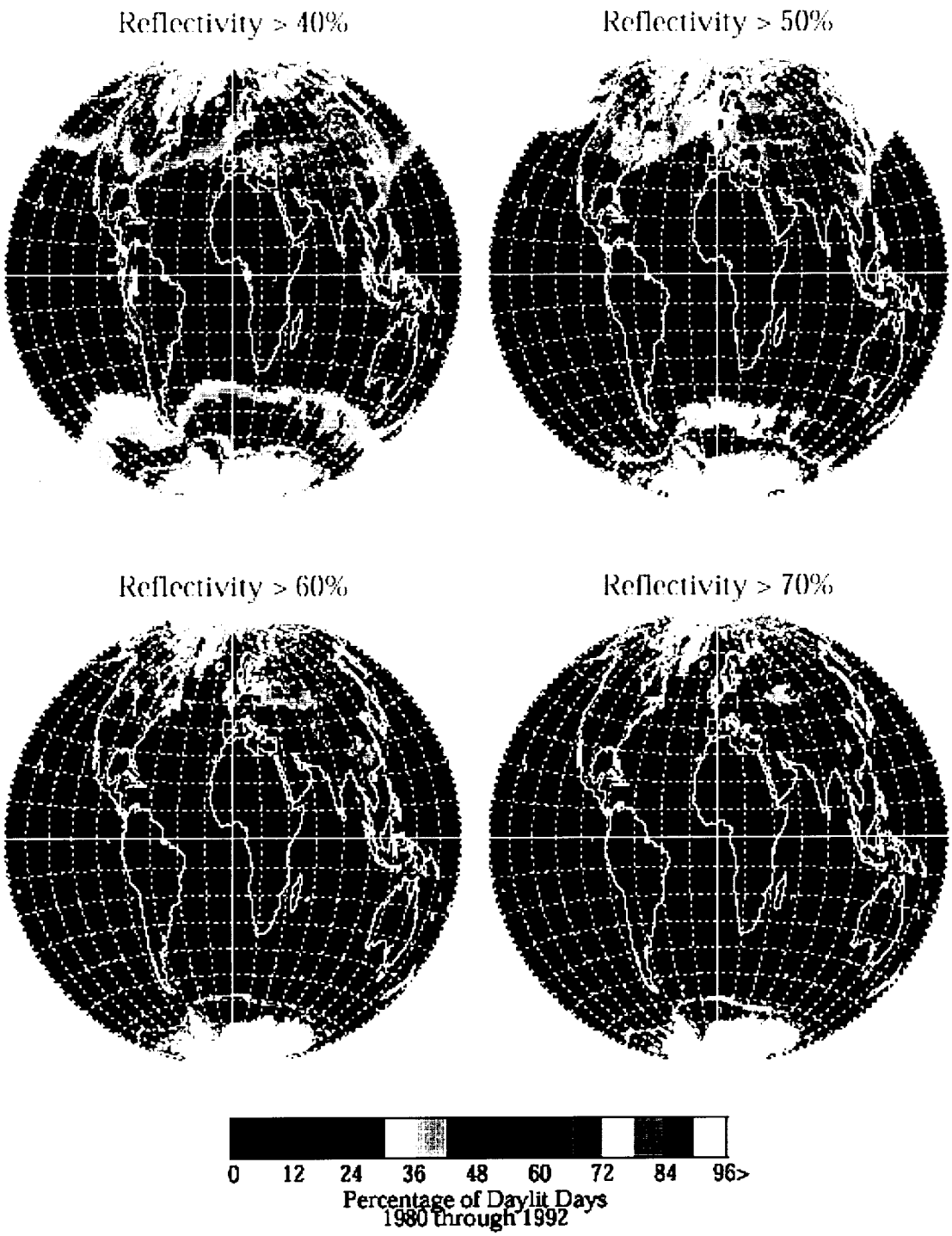

Plate 5 **The percentage of days with reflectivity > 40, 50, 60, or 70% for the period 1980 to 1992. Areas poleward of the Arctic or Antarctic circle are normalized to number of sunlit days.**

Over much of North America, Europe, and Russia there is an optically thick band of clouds (R>40%) or snow present for about half of the year. Also visible in the R>70% and R>60% panels (blue, 24 to 30% occurrence) is the likely US "Lake Effect" band of snow and clouds extending eastward from the Chicago area into New England. The blue color is a peak value for occurrence of cloudy days at high reflectivity (27% of the year) in a background band of 15% of the year. At lower reflectivities, R> 40% and R>50%, the ability to distinguish this effect disappears.

Seasonal Frequency of Occurrence

The frequency of occurrence for clear-sky data can be organized by season, as shown in Plate 6. The most obvious changes are those caused by the interaction of ocean currents with the atmosphere.

The clear-sky frequency distributions over the oceans mark out the circulation patterns of underlying currents. The largest ocean current interaction occurs when warm or cold water currents come in contact with cold or warm air, respectively. The clearest examples of this are for the cold-water California and Humboldt currents during their respective summer months. For example, in the Southern Hemisphere the cold-water Humboldt current circulates from west to east until it strikes the west coast of South America where it turns northward and eastward (Peru current). In the winter, July, the current flows at mid-latitudes, turns north well before striking land, and forms a loop flowing eastward along the equator. The winter and spring month increase in number of cloudy days (see Plate 6 for JJA and SON) follows this pattern, but with the clouds displaced north of the equator driven by easterly winds forced slightly north of the equator by land features. Similar cloud and clear-region patterns are seen in the ISCCP cloud data set [Rossow, 1993c]. For example, the extremely clear region over the equatorial Pacific Ocean (near 160°W) is seen in both the TOMS and ISCCP data sets.

Interannual Variability

The largest interannual changes in reflectivity occur during the El Nino years, with the strongest of these (1979 to 1992) being 1982. The large clear area in the equatorial region of the Pacific Ocean (R<15% for 85% of 1981) gradually becomes more cloudy (R<15% for 50% of 1983), and then clears again after the El Nino period (i.e., 1985 is very similar to 1981). At the same time, the thin cloud band at 9°N is a minimum in 1983 and fully recovers by 1984. A similar cloud pattern, with its largest variability during El Nino years, lies off of the west coast of southern Africa. Most large-scale cloud features change little from year to year, except for moving slightly relative to ground locations. An example of an exception is the region of reflectivity increase occurring off the west coast of South America near northern Chile probably related to changes in the Humboldt current. In addition, there are only small reflectivity changes from year to year in zonal averages [Herman et al., 2000], other than for high latitude regions in both hemispheres where there have been significant long-term increases.

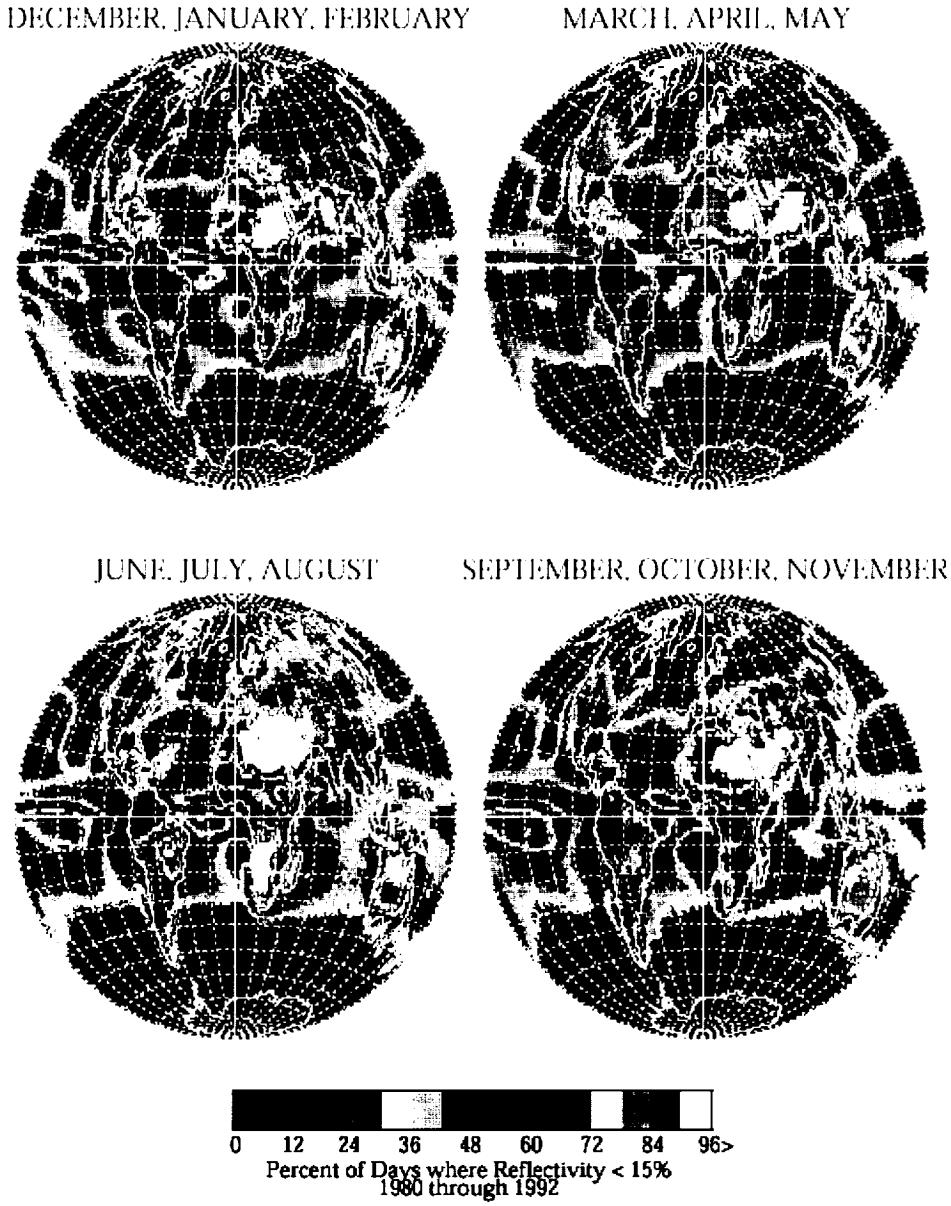

Plate 6 Average (1980 to 1992) seasonal distribution of clear-sky days when the reflectivity is less than 15%. June, July and August=JJA, September, October, November=SON, December, January, February=DJF, March, April, May=MAM.

Summary

The persistent features of the Earth's clouds over land and oceans are shown using 14 years of 380 nm radiance measurements from TOMS. The radiance measurements, converted into the combined reflectivity of the Earth's surface and atmospheric clouds and aerosols, shows the influence of the ocean currents and major wind systems on cloud formation. Because both land and ocean surfaces are dark when viewed at 380 nm (4 to 8% reflectivity), even small amounts of cloud cover can be distinguished from clear-sky conditions. The result is that the most commonly observed scene for most regions of the Earth contains a light haze of about 2 to 4% above the ground reflectivity. This haze produces additional reflection of radiation back to space that should be taken into account when computing the energy balance of the Earth (UV to near infrared). Since the haze occurs in the lowest portion of the troposphere, the combined reflectivity for haze plus the surface should be used as the boundary value for space-based observations of the clear-sky Earth's atmosphere. Where reflectivity data are not available, the mode values can be used as a reflectivity climatology of the Earth's boundary layer for UV radiation problems in the atmosphere.

In most regions of the Earth, there are a large number of days each year when the reflectivity is low (less than 10 to15%). Since surface reflectivities are 2 to 5%, this indicates that the skies are mostly cloud free, but may contain water haze or other tropospheric aerosols. Certain areas (e.g., Australia, southern Africa, portions of northern Africa) are cloud-free more than 80% of the year, which exposes these regions to larger amounts of UV radiation than at comparable latitudes in the Northern Hemisphere. Regions over rain-forests, jungle areas, and most ocean areas have some cloud cover more than 80% of each year. Most notable are the forest areas of northern South America, southern Central America, and the jungle areas of equatorial Africa. Most ocean areas with surface reflectivities from 2 to 8% have some cloud or aerosol cover more than half of each year (R>10%).

Seasonal- and annual-average cloud formation shows patterns that correspond to the underlying cold-water ocean currents. The largest of these effects follow the California and Humboldt currents off of the west coasts of the US and South America, respectively, and the warm-water Gulf Stream in the northern Atlantic. A similar smaller cloud formation region follows an ocean current in the Atlantic off of the western coast of Africa..

References

Allen, D.R., M.R. Schoeberl, and J.R.Herman, Trajectory modeling of aerosol clouds observed by TOMS,, J. Geophys. Res., 104,27461-27471, 1999.

Eck,T.F., P.K.Bhartia, P.H. Hwang, and L.L. Stowe, Reflectivity of Earth's surface and clouds in ultraviolet from satellite observations, J. Geophys. Res., 92, 4287-4296, 1987.

Eck,T.F., P.K.Bhartia, and J.B.Kerr, Satellite estimation of spectral UVB irradiance using TOMS derived total ozone and UV reflectivity, Geophys. Res. Lett., 22, 611-614, 1995.

Harrison et al., in "Atlas of satellite observations related to global change", Edited by R.J. Gurney, J.L. Foster, C.L. Parkinson, Cambridge University Press, 1993

Herman, J.R. and D.Larko,, Low ozone amounts during 1992-1993 from Nimbus-7 and Meteor-3/TOMS", *J.Geophys. Res.*, **99**, 3438-3496, 1994.

Herman, J.R. and E. A. Celarier, Earth Surface Reflectivity Climatology at 340 nm to 380 nm from TOMS Data, J. Geophys. Res.102, 28003-28011, 1997.

Herman, J.R., P.K. Bhartia, O.Torres, C. Hsu, C. Seftor, E. Celarier, Global Distribution of UV-Absorbing Aerosols From Nimbus-7/TOMS Data", J.Geophys. Res., **102**, 16,911-16,922, 1997.

Herman, J.R., N. Krotkov, E. Celarier, D. Larko, and G. Labow, The Distribution of UV Radiation at the Earth's Surface From TOMS Measured UV-Backscattered Radiances, J. Geophys. Res. 104, 12059-12076, 1999.

Herman, J. R., D. Larko, and J. Ziemke, Changes in the Earth's Global UV Reflectivity from Clouds and Aerosols", submitted to, J. Geophys. Res., 2000.

Hsu, N. C., J.R Herman, and C. Weaver, Determination of Radiative Forcing of Saharan Dust Using Combined TOMS and ERBE Data", submitted to J. Geophys. Res., 1999.

Hsu, N. C., J.R. Herman, O. Torres,B, N. Holben, D. Tanre, T. F. Eck, A. Smirnov, B. Chatenet, and F. Lavenu, Comparisons of the TOMS aerosol index with sun photometer aerosol optical thickness, J. Geophys. Res., 104, 6269-6279, 1999.

Krotkov,N., J.R. Herman., P.K. Bhartia, Z. Ahmad, V. Fioletov, Satellite estimation of spectral surface UV irradiance 2: Effect of horizontally homogeneous clouds, submitted to J. Geophys. Res., 2000.

Lubin, D., E.H. Jensen, and H.P. Gies, Global surface ultraviolet radiation climatology from TOMS and ERBE data, J. Geophys. Res., **103**, 26061-26092, 1998.

McPeters, Richard D, P. K. Bhartia, A. J. Krueger, J.R. Herman, C. G. Wellemeyer, C.J. Seftor, G. Jaross, O. Torres, L. Moy, G. Labow, W. Byerly, S. L. Taylor, T. Swissler, and R.P. Cebula, Earth Probe Total Ozone Mapping Spectrometer (TOMS) Data Products User's Guide, NASA Technical Publication, 1998-206895, Goddard Space Flight Center, 1998.

Rossow, W.B. and L.C. Garder, Cloud Detection Using Satellite Measurements of Infrared and Visible Radiances for ISCCP, J. Climate, **6**, 2341-2369, 1993a.

Rossow, W.B. and L.C. Garder, Validation of ISCCP Cloud Detection, J. Climate, **6**, 2370-2393, 1993b

Rossow, W.B., Clouds, in "Atlas of satellite observations related to global change", Edited by R.J. Gurney, J.L. Foster, C.L. Parkinson, Cambridge University Press, 1993c.

Torres, O., J.R. Herman, P.K. Bhartia, and Z. Ahmad, Volcanic aerosols, 1994 "Properties of Mt. Pinatubo Aerosols as derived from Nimbus-7 TOMS measurements", *J. Geophys. Res.*, **100,** 14043-14055, 1995.

Torres, O., P.K. Bhartia, J.R.Herman, and Z. Ahmad, Derivation of Aerosol Properties From Satellite Measurements of Backscattered Ultraviolet Radiation. Theoretical Basis", J.Geophys. Res., 103, 17099-17110, 1998.

Willson, Solar Irradiance, in "Atlas of satellite observations related to global change", Edited by R.J. Gurney, J.L. Foster, C.L. Parkinson, Cambridge University Press, 1993.

WMO, UV Radiation an the Earth's Surface" Chapter 9, J. R. Herman, McKenzie, S. Diaz, J. Kerr, S. Madronich, and G. Seckmeyer, WMO 1999, UNEP/WMO Scientific Assessment of Ozone Depletion: 1999, edited by D. L. Albritton, R. T. Watson, and P. J. Aucamp, *WMO Global Ozone Res. and Monit. Proj.*, Geneva, 1999.

Figure Captions

Figure 1 The values of reflectivity and their frequency of occurrence over eastern Australia and central Virginia, USA. Reflectivities are represented in percent (0 to 100).

Figure 2 The frequency of occurrence of different reflectivity values at locations in Germany, Nevada, Greenland, and in Niger. Reflectivity expressed in percent.

Figure 3 Frequency of occurrence of reflectivity values over ocean areas.

Figure 4 Annual mean zonally averaged reflectivity for the period 1980 to 1992. The error bars are 2 standard deviations.

Figure 5 The relationship between cloud optical depth τ and reflectivity R for a uniform cloud field viewed from the nadir observing position from the satellite. The curves are for 3 solar zenith angles, 0, 46, and 70 degrees.

Plate 1 TOMS reflectivity and aerosol index for 09 Sept 1987. The blue and tan colors represent water and land. The upper panel has the aerosol index superimposed on top of the reflectivity data, while the lower panel is just the reflectivity data.

Plate 2 Monthly average reflectivity in percent for the years 1980 - 1992 for January, April, July, and October.

Plate 3 The areas of the Earth where there are at least an average of 20 cloud-free days per year (i.e., reflectivity less than 10%, bottom, or 15%, top). Areas colored red are cloud free about ½ the time.

Plate 4 The percentage of days with reflectivity > 70% for the period 1980 to 1992. Areas poleward of the Arctic or Antarctic circle are normalized to number of sunlit days.

Plate 5 The global distribution of the most probable value of reflectivity for each TOMS scene on a 1° x1.25° grid for values of R between 0 and 30%. The most probable value corresponds to the large maximum in the reflectivity histogram (see Figures 2, 3, and 4)

Plate 6 Average (1980 to 1992) seasonal distribution of clear-sky days when the reflectivity is less than 15%. June, July and August=JJA, September, October, November=SON, December, January, February=DJF, March, April, May=MAM.

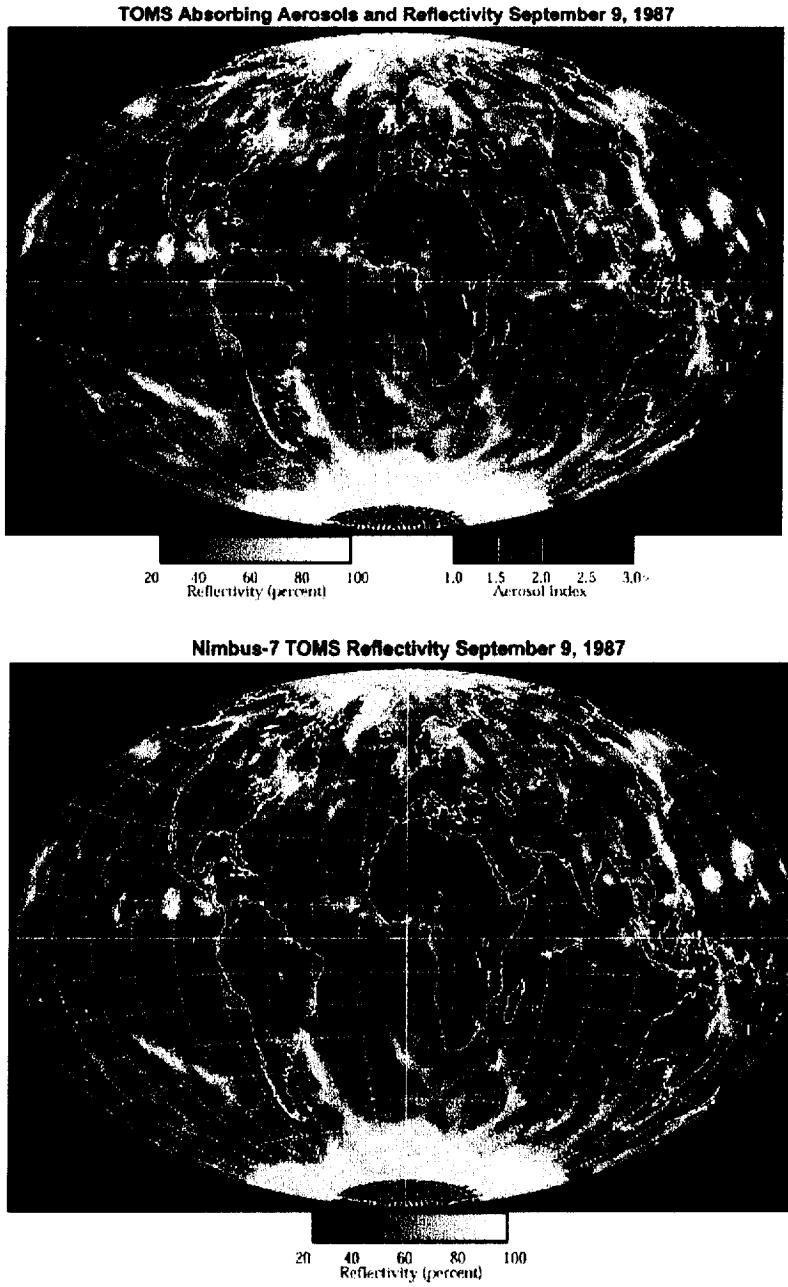

Plate 1 TOMS reflectivity and aerosol index for 09 Sept 1987. The blue and tan colors represent water and land. The upper panel has the aerosol index superimposed on top of the reflectivity data, while the lower panel is just the reflectivity data.

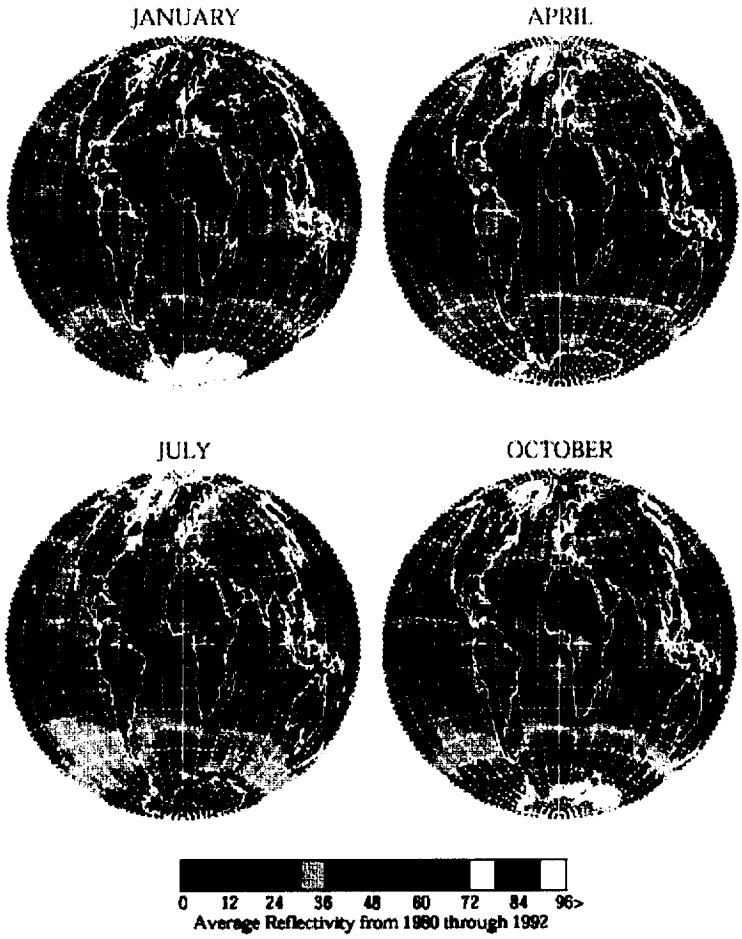

Plate 2 Monthly average reflectivity in percent for the years 1979 - 1992 for January, April, July, and October.

Reflectivity Value of Maximum Occurrence for the period 1980 through 1992

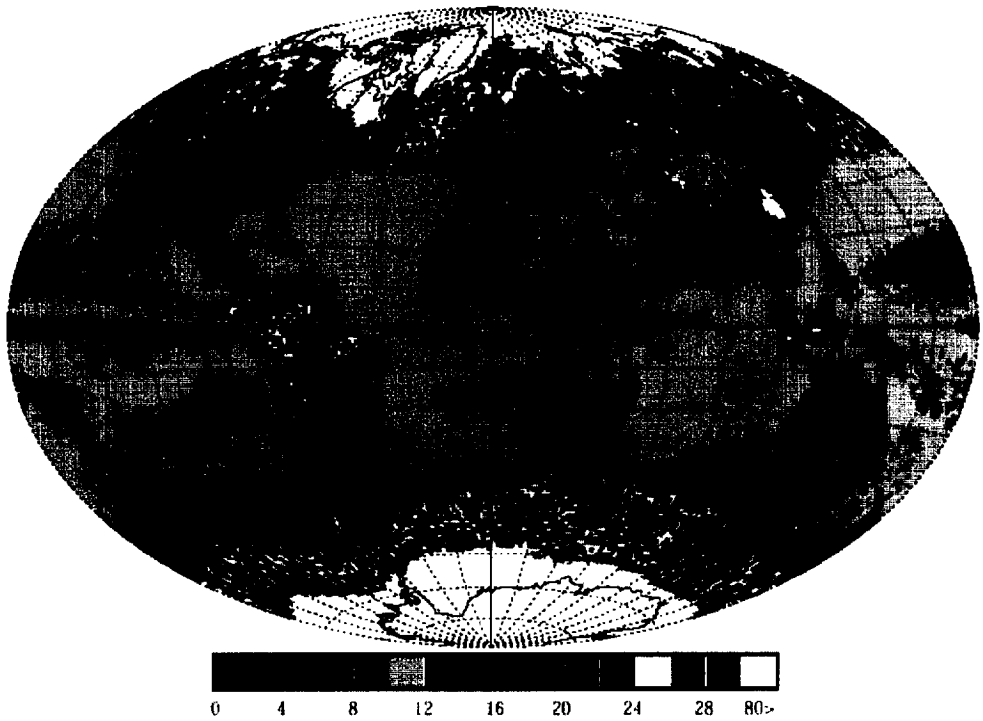

Plate 3 The global and seasonal distributions of the most probable annual value of reflectivity (mode) for each TOMS scene on a 1° x1.25° grid for values of R between 0 and 30%. All values over 30% are in the last color box (white). The most probable value corresponds to the large maximum in the reflectivity histogram (see Figures 1, 2, and 3)

Average Number of Days per Year where Reflectivity < 15% for 1980 through 1992

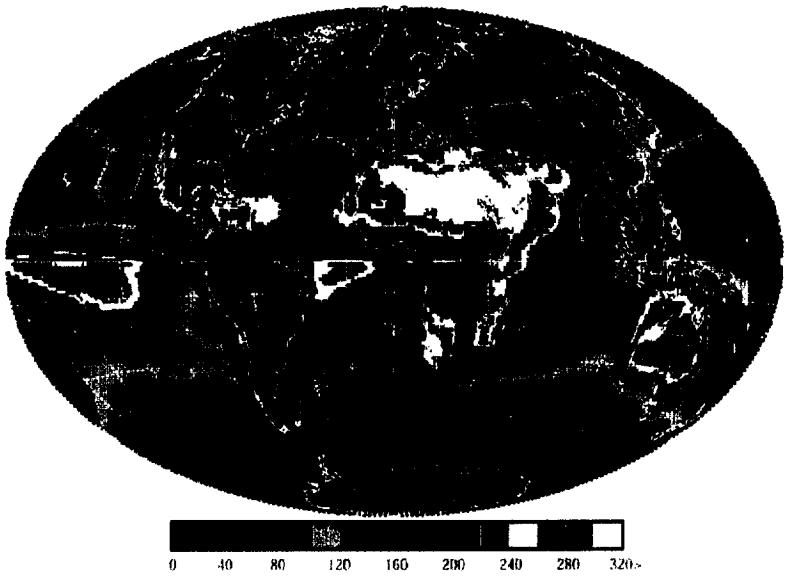

Average Number of Days per Year where Reflectivity < 10% for 1980 through 1992

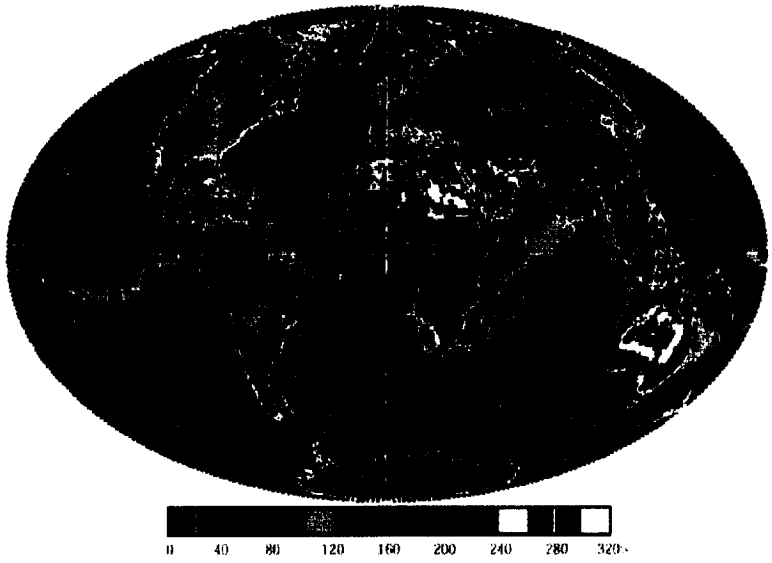

Plate 4 The areas of the Earth where there are at least an average of 20 cloud-free days per year (i.e., reflectivity less than 10%, bottom, or 15%, top). Areas colored red are cloud free about ½ the time.

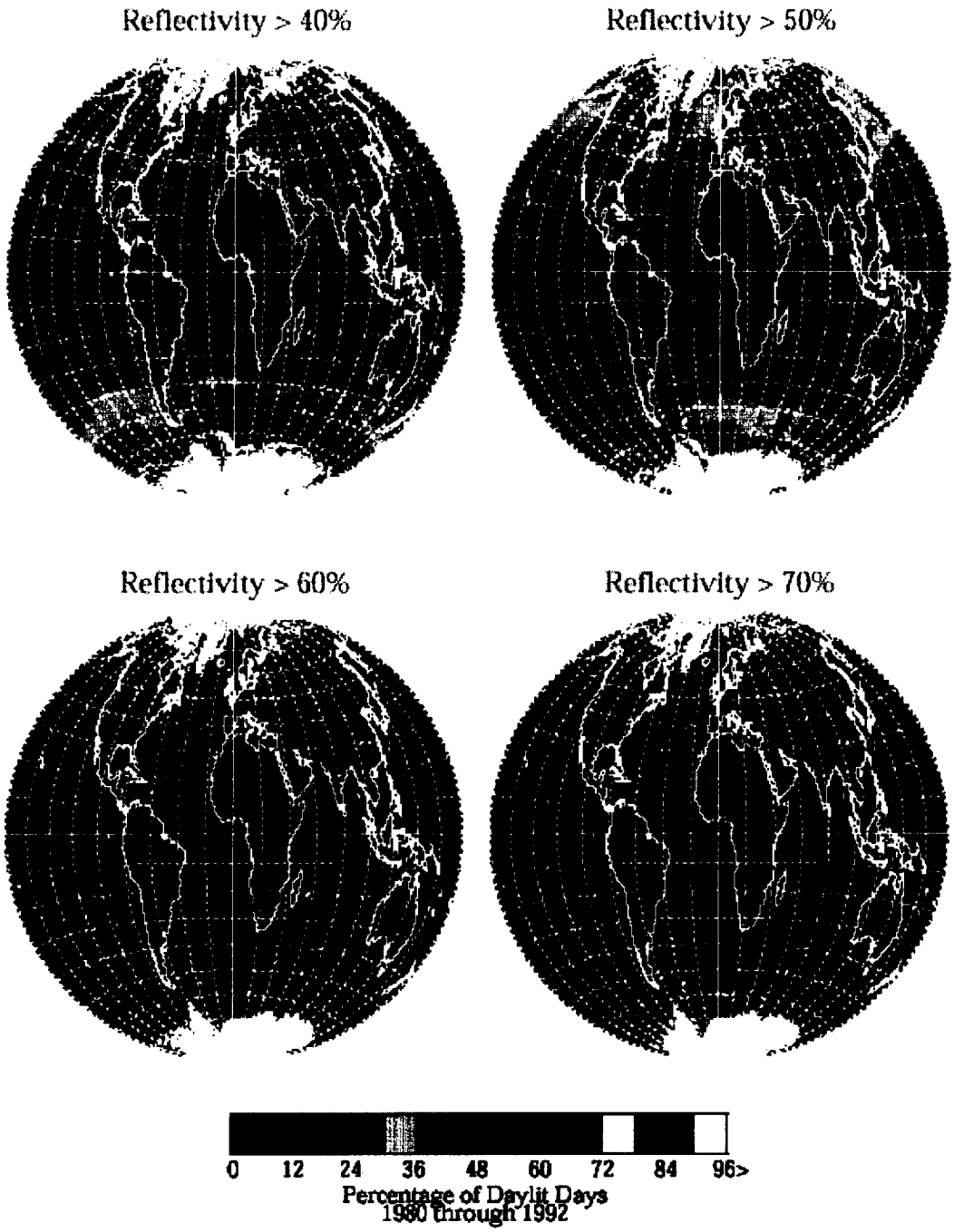

Plate 5 The percentage of days with reflectivity > 70% for the period 1980 to 1992. Areas poleward of the Arctic or Antarctic circle are normalized to number of sunlit days.

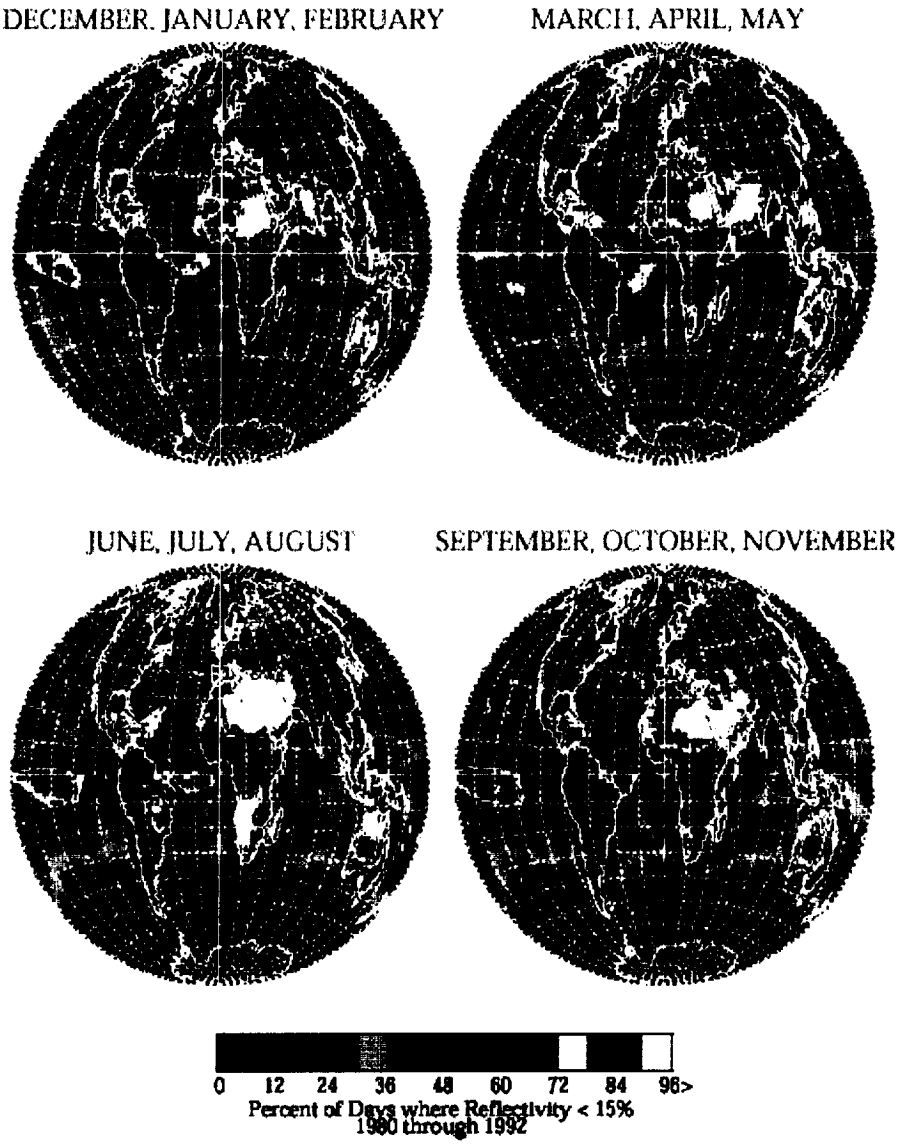

Plate 6 Average (1980 to 1992) seasonal distribution of clear-sky days when the reflectivity is less than 15%. June, July and August=JJA, September, October, November=SON, December, January, February=DJF, March, April, May=MAM.